



Luminescence peculiarities of polyamide-6 α and γ forms

M. V. Vasnetsov¹ · V. V. Ponevchinsky¹ · D. O. Plutenko¹ · G. V. Klishevich¹ · A. A. Mitryaev¹ · O. I. Gudymenko² · V. P. Kladko²

Received: 5 October 2020 / Accepted: 2 March 2021 / Published online: 19 March 2021
© The Author(s), under exclusive licence to Springer-Verlag GmbH Germany, part of Springer Nature 2021

Abstract

Persistent time-delayed luminescence was observed in bulk polymer Polyamide-6 (nylon 6) samples at room temperature. Using X-ray 2Θ -diagnostics we have separated two crystalline forms of the material which exhibit serious differences in their time-delayed luminescence properties. Whilst for the α -form the afterglow temperature threshold is at the range of 100 °C, the γ -form samples require cooling to about -20 °C for the effect becomes observed by eye. The afterglow relaxation traces are highly reproducible and we extracted the Becquerel law function (compressed hyperbola) for them. The conclusion derived on the origin of the effect is the photoinduced charge recombination process. A theoretical model is presented for the explanation of the experimental results.

1 Introduction

There is a big literature to date devoted to the luminescence of organic (particularly polymer) materials and a large scope of experimental studies and theoretical approaches to the problem [1–4]. However, the most attention was directed to the effects associated with some material-related parameters, i.e. molecular structure. In this view, our goal is to distinguish a general property inherent to materials of different origin. As an object, we have chosen easy available Polyamide-6 (PA-6) in two modifications [5]. The interest to commercially produced Polyamide-6 material is usually connected with the characterization of fibers and yarn [6, 7]. Oppositely, our study is devoted to bulk solid polymer substance with particular attention to its photophysics properties. Recently we reported on the effect of a persistent afterglow observed at room temperature with PA-6 illuminated in UV range [8]. As the origin of the effect was quite unclear, some new methods were applied to understand the issue. With the use of X-ray 2Θ -treating we have found an evident correlation between the microscopic crystalline structure of

the material and the luminescence properties of PA-6 samples. The α -form samples demonstrate persistent afterglow (several seconds duration) at room temperature, in contrast to γ -form samples which start the visual glowing at about 250 K. The temperature dependence was checked for both crystalline forms.

We applied a technique for isolation of the afterglow signal and registered temporal decay function in accordance with the Becquerel law (compressed hyperbola). The analysis performed gives an explanation for the hyperbolic delayed luminescence function.

2 Experiment

An example of the time-delayed luminescence signal observed at room temperature conditions is shown in Fig. 1. We used pulse N_2 laser operating at 337 nm wavelength with pulse duration 9 ns to excite PA-6 samples. Luminescence was collected by a quartz lens and the signal was cleaned from a scattered UV pump with a glass filter. A photomultiplier with a time resolution better 1 μ s was used to register the signal.

The short laser pulse permits detection of fast fluorescence response and possible time-delayed emission. Indeed we have detected a sharp peak and extremely long “tail” of the afterglow. Even with the temperature increase, the afterglow was still detected as shown in Fig. 1a. The single-shot relaxation function appeared non-exponential and the best fit

✉ M. V. Vasnetsov
mvas@iop.kiev.ua

¹ Institute of Physics, National Academy of Sciences of Ukraine, Prospect Nauki 46, Kyiv 03028, Ukraine

² V. E. Lashkaryov Institute of Semiconductor Physics, National Academy of Sciences of Ukraine, Prospect Nauki 41, Kyiv 03028, Ukraine

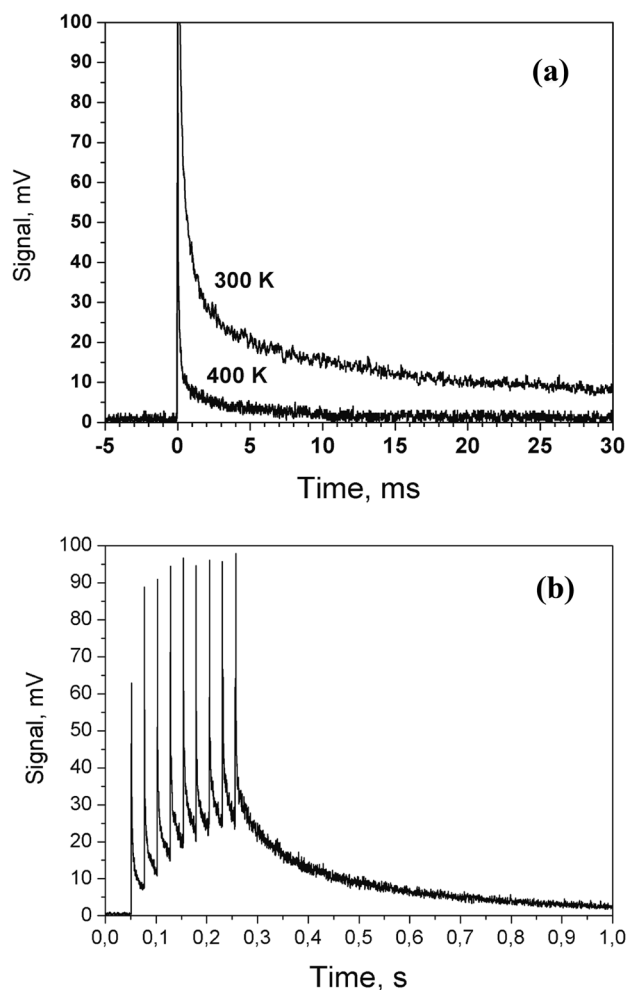


Fig. 1 **a** Typical luminescence response of PA-6 sample on a short excitation pulse from N₂ laser (337 nm wavelength) at room temperature (300 K) and under heating to 400 K. **b** Accumulation of the afterglow signal under pulse-periodic excitation (9 pulses from N₂ laser, 50 Hz repetition rate)

was found in a form of hyperbola. (Below we shall examine this point in more details).

In the pulse-periodic regime (repetition rate 50 Hz) the following pulses contribute conjointly to the time-delayed signal which is fairly seen by eye at room temperature during several seconds after switching the pump off (Fig. 1b). The signal accumulation does not happen for a heated sample as the relaxation time amounted to about 10 ms for the 400 K temperature.

However, samples of PA-6 taken from different sources behave in a different manner: some exhibit the same time-delayed luminescence at room temperature, other required cooling for the effect to occur. To explain the strange contradiction we have analyzed the samples along with their microscopic structure.

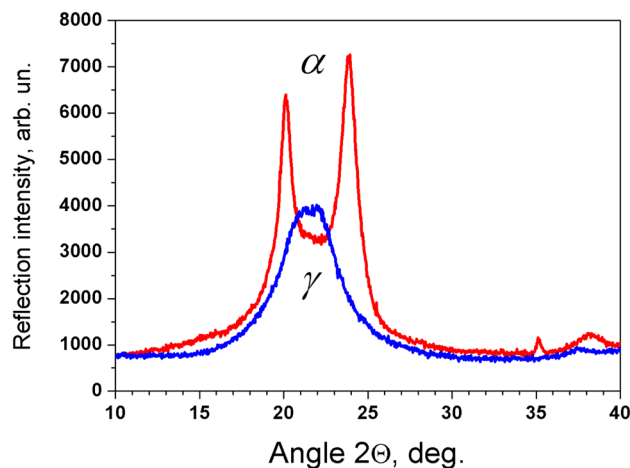


Fig. 2 Wide-angle X-ray diffraction pattern of polyamide-6 samples in α and γ forms as indicated

2.1 X-ray diagnostics and luminescence spectra

As it is known, two crystalline modifications exist in PA-6 which differ in the morphology of molecular chains packing [9]. In this view, we have separated the samples along with their crystalline morphological forms with the aid of X-ray diagnostics (Bragg reflection 2Θ -technique). The results obtained for the tested objects are shown in Fig. 2: samples of the γ -crystalline phase possess well defined single reflection peak at about 21.5° , whereas the samples of the α -crystalline phase show two sharp reflection peaks at 20.13° and 23.85° .

The detected difference in a crystalline form thus determines the temperature threshold for the afterglow effect: α -form samples give a persistent afterglow observing at room temperature and γ -form samples do not. Moreover, the luminescence spectra appeared also quite different for these forms.

The samples' luminescence was tested with HITACHI MPF-4 spectrofluorimeter at room temperature with the excitation wavelength range from 250 to 400 nm. This choice was conditioned by the width of the examined luminescence spectrum which occupies near UV and practically the whole visible range. We detected for the α -form samples the existence of two luminescence bands, one with the maximum at 340 nm and another with 390 nm with the elongation to 600 nm. As seen in Fig. 3 the luminescence of α -form sample exhibits a switching from the 340 nm band to the 390 nm band in a short interval of the excitation wavelength between 300 and 310 nm.

Similar measurements were performed with γ -form samples. We did not detect the switching between the separate luminescence bands but instead a gradual shift of the

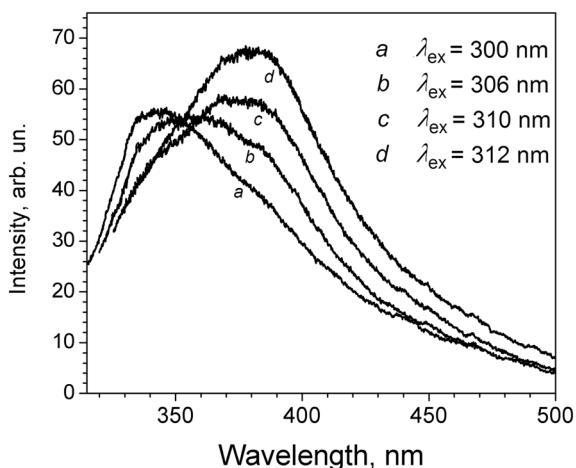


Fig. 3 Switching of the luminescence bands observed with α -form sample at the excitation wavelength range from 300 to 310 nm

maximum from the near UV to the visual spectrum range (Fig. 4).

We note the results obtained for the α -form sample are in good coincidence with the literature data [10]. Relating to the observed luminescence spectra, the afterglow effect with the excitation in the region 300–400 nm releases the emission in the band 400–600 nm.

2.2 Time-delayed luminescence inspection

The first observation of the afterglow in Polyamide-6 sample with a pulse N_2 laser stimulated the development of a more advanced technique for the effect inspection. Instead of a short-pulse source, we applied periodically switched UV LED or

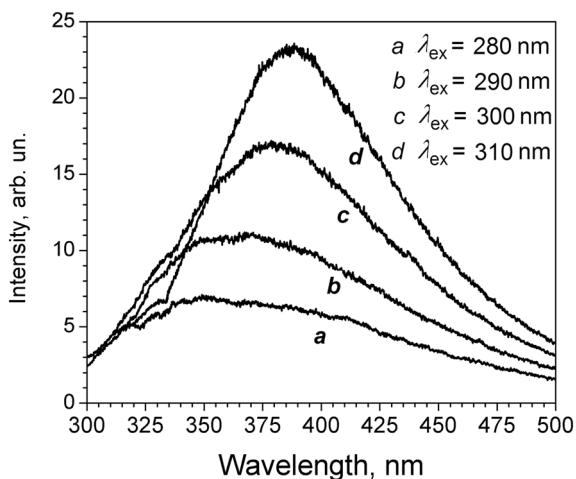


Fig. 4 Luminescence band shift observed with the variation of the excitation wavelength in the range from 280 to 310 nm observed with γ -form sample

diode laser. To isolate a relatively small signal of the time-delayed emission (with respect to the bright fluorescence) we used a shutter which blocks the input to the photomultiplier at the moments of the pulse pump. Thus the shutter closes the window during the pump pulses and opens it in the intervals between the pulses, therefore the only afterglow signal can be registered when the window is open. In this way pure afterglow signal will be detected without the fluorescence peaks.

The experimental setup is schematically depicted in Fig. 5. To carry out temperature measurements, a cryostat with a sample inside was used. UV radiation is concentrated on the sample with the lens L_1 and the luminescence is collected with the lens L_2 . The color glass filter in front of the photomultiplier window blocks the scattered UV pump radiation.

The resulting oscilloscope trace is shown in Fig. 6. The rise of the afterglow signal is seen (accumulation of the excitation) until reaching a saturated value as well as the decay after switching the pump off. (Periodically closing window gives the control of the photomultiplier background dark noise).

The reliability of the experiment permits to resolve with high accuracy the temporal function of the afterglow relaxation. (We note for a long excitation time and accumulation of excitation in the material the temporal characteristic of the afterglow differs from registered in the case of a single short pulse (Fig. 1)). An analysis gives the fitting parameter $\kappa = 1.08$ for the relaxation function in the form of compressed hyperbola (Becquerel law [11])

$$S(t) = \frac{S_0}{(t + t_0)^\kappa} \tag{1}$$

S_0 and t_0 are experimental parameters.

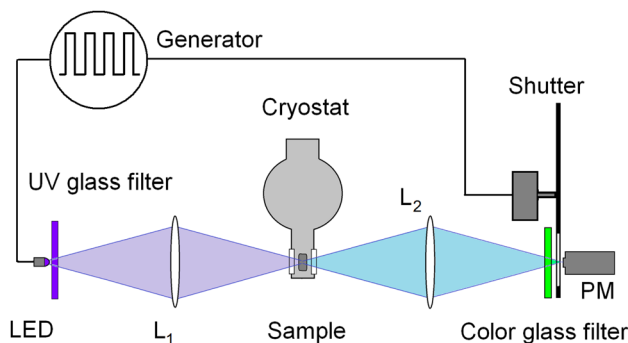


Fig. 5 Experimental scheme composed from the excitation LED (374 nm emission) or laser diode (407 nm) operating in a pulse-periodic regime (emission spectrum is rectified with a UV glass filter), lenses L_1 and L_2 , sample in a cryostat, and a detector (photomultiplier) with a color glass filter cutting off the scattered pump radiation. The shutter closes the photomultiplier (PM) window at the moments of the excitation pulses and opens it in the interval between them

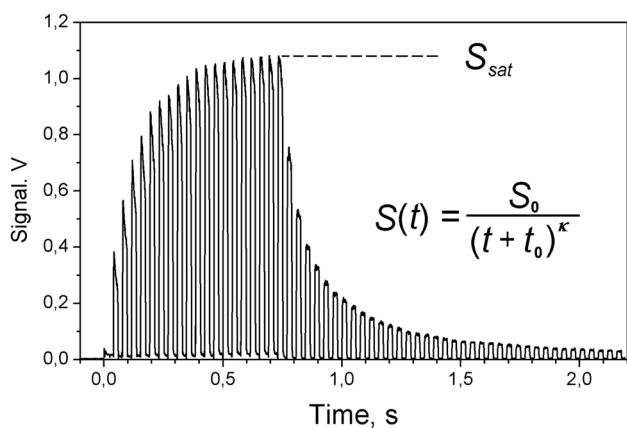


Fig. 6 Experimentally recorded with the aid of the shutter system time-delayed luminescence signal. Excitation from a diode laser (407 nm) lasts to 0.7 s until the saturated level S_{sat} is reached, then the relaxation of the afterglow signal is detected with a hyperbolic function

2.3 Temperature dependence

The elaborated technique permits also precise measurements of the afterglow temperature dependence and the determination of the effective threshold. The value S_{sat} was measured in the same experimental environment with controllably varied sample temperature. In the range from 20 to 120 °C we observed first a decrease of the magnitude S_{sat} with some stabilization in the interval 40–80 °C until the final decrease which is caused by the diminishing of the relaxation time to the value less than the period of the pulse train (Fig. 6). The interval between the excitation pulses amounted to 12 ms, in these conditions the signal accumulation does not take place with the temperature rise to 80 °C. Of course with shorter intervals the signal decrease will occur at higher temperature. Vice versa with the interval 22 ms the corresponding temperature was found 60 °C as seen in Fig. 7.

The examples of the shape of the relaxation function obtained for α -form samples are given in Fig. 8 for the peak-normalized plots corresponding to the measurements at 25 and 125 °C. This picture qualitatively explains the disappearance of the afterglow seen by the eye: the relaxation time diminishes to about 10 ms which is less than an eye’s recognition time. In this view the temperature threshold for the afterglow observed by eye is close to 50 °C.

We have measured also the temperature dependence for γ -form samples with the use of a cryostat as shown in the experimental scheme (Fig. 4). The results presented in Fig. 9 show very similar behaviour with the signal decrease at the room temperature range for α -form. The threshold occurs at about 0 °C as it is seen.

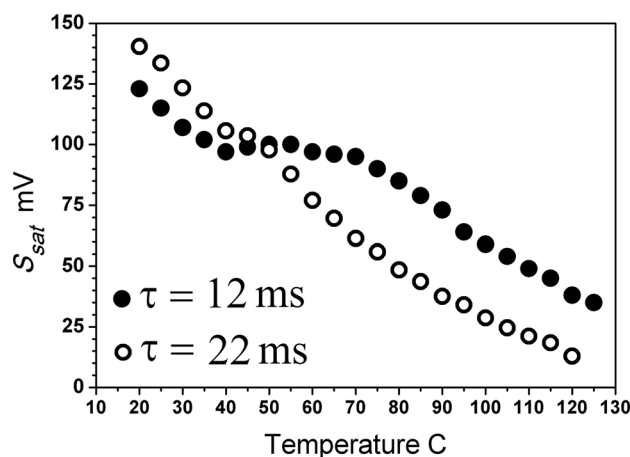


Fig. 7 Temperature dependence of the saturated signal S_{sat} for a pulse-periodic excitation (closed circles, pulse duration 12 ms, the interval between pulses $\tau = 12$ ms, open circles, pulse duration 44 ms, the interval between pulses $\tau = 22$ ms) for α -form sample

2.4 Afterglow spectrum detection

The experimental setup also can be used for the detection of the afterglow spectrum. As the excitation source in these measurements, we accepted UV LED with the emission band at 368 nm. The choice of α -form sample does not require sample cooling and simplified the measurements at laboratory temperature conditions. With the periodically open window, a relatively weak afterglow signal was analyzed by Ocean Optics spectrometer. The detected spectrum is presented in Fig. 10. A comparison with the fast fluorescent spectrum (time window 10^{-8} s) obtained for the same

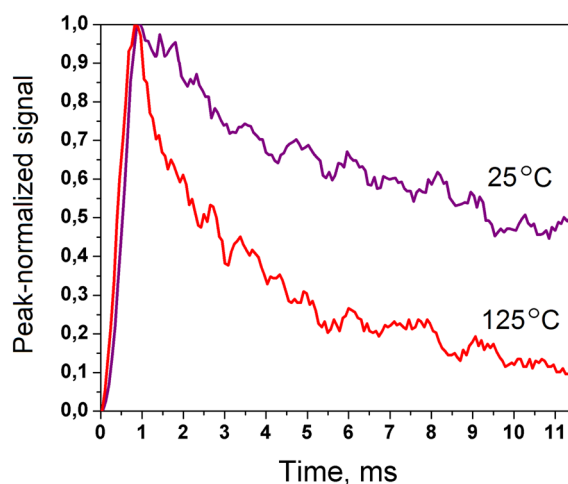


Fig. 8 Relaxation of the measured afterglow signal, for room temperature (25 °C) and heated sample (125 °C), for the α -form PA-6 sample

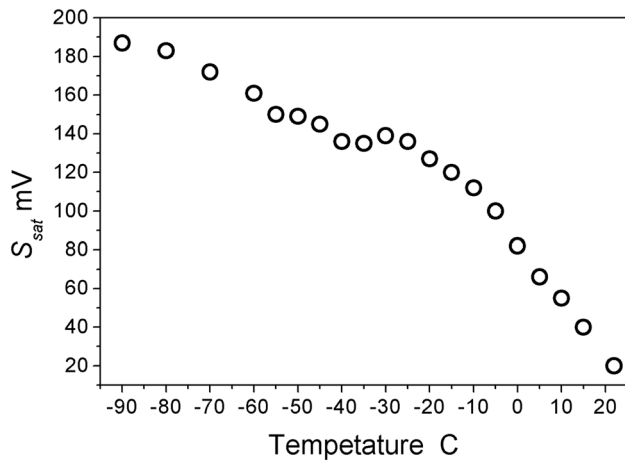


Fig. 9 Temperature dependence of the saturated afterglow signal S_{sat} measured for γ -form sample. The interval between excitation pulses amounts to 20 ms

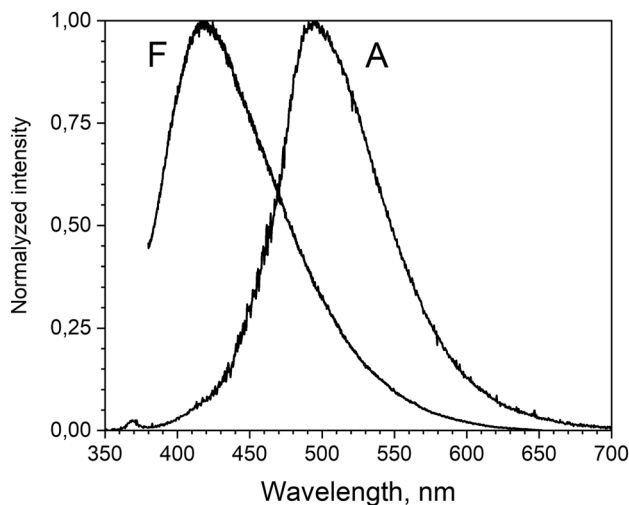


Fig. 10 The afterglow spectrum (A) and fast-response fluorescence spectrum (F) recorded with the excitation at the wavelength 368 nm

excitation wavelength 368 nm with the use of HITACHI MPF-4 spectrofluorimeter is given.

3 Analysis and discussion

As follows from our previous considerations [8], the afterglow effect is originated owing to the recombination of photoinduced charges with nearly continuum energy distribution. The excitation process can be considered therefore as an accumulation of the electrons on the traps which number (per molecule) can be limited. During the following relaxation, the trapped electrons can recombine with holes. Thus we

consider the luminescence process as a transition of a trapped localized electron to a trapped localized hole in the conditions of extremely low mobility of the charges involved and their random spatial distribution.

The model of time-delayed emission can be constructed on the assumption of existence of localized states with different energy levels. Let us assume also that the holes have tight localization. The trap is defined by a sphere with the radius a and energy $U(r)$ where r is the modulus of the radius vector \mathbf{r}

$$U(\mathbf{r}) = \begin{cases} U_e, & |\mathbf{r}| \leq a \\ 0, & |\mathbf{r}| > a \end{cases} \quad (2)$$

The corresponding Schrodinger equation for a trapped electron is written as

$$\left(-\frac{\hbar^2 \Delta}{2m_e} + U(\mathbf{r}) \right) \Psi_i^{(0)} = E \Psi_i^{(0)} \quad (3)$$

We can find the solution for an isolated trap outside the sphere in a form of superposition of functions $\psi_l^{(m)}(\mathbf{r})$

$$\psi_l^{(m)}(\mathbf{r}) = Y_l^{(m)}(\theta, \varphi) R_l(r), \quad (4)$$

where $Y_l^{(m)}$ are spherical functions with indices l and m

$$Y_l^{(m)}(\theta, \varphi) = \frac{1}{2\pi} e^{im\varphi} \Theta_{lm}(\theta) \quad (5)$$

and

$$\Theta_{lm}(\theta) = (-1)^{\frac{|m|-m}{2}} \left[\frac{2l+1}{2} \frac{(l-|m|)!}{(l+|m|)!} \right]^{1/2} P_l^{|m|}(\cos\theta), \quad (6)$$

where P_l^m is the Legendre polynomial. Radial function $R_l(r)$ satisfies the equation

$$\left[\frac{\partial^2}{\partial r^2} + \frac{2}{r} \frac{\partial}{\partial r} - \frac{l(l+1)}{r^2} \right] R_l(r) = -\frac{2m_e E}{\hbar^2} R_l(r) \quad (7)$$

For negative E Eq. (7) transforms to a modified Bessel equation. The solution is expressed via Bessel function of second order (Macdonald function) of a fractional order $K_{l+1/2}(\kappa r)$

$$R_l(r) = a_l (\kappa r)^{-1/2} K_{l+1/2}(\kappa r), \quad (8)$$

where a_l is a constant and

$$\kappa = \frac{(2m_e |E|)^{1/2}}{\hbar}. \quad (9)$$

Asymptotic behavior of the Macdonald function at the limit $\kappa r \rightarrow \infty$ takes the form

$$K_{l+1/2}(\kappa r) \rightarrow \frac{1}{\sqrt{2\pi}} \frac{e^{-\kappa r}}{\sqrt{\kappa r}}, \quad (10)$$

what gives the result

$$R_l(r) \rightarrow \frac{\alpha_l}{\sqrt{2\pi}} \frac{e^{-\kappa r}}{\kappa r}, \quad (11)$$

and therefore

$$\Psi_i^{(0)} \propto \frac{e^{-\kappa r}}{\kappa r} \Big|_{\kappa r \rightarrow \infty}. \quad (12)$$

According to the Fermi's golden rule a probability for the transition to a low-energy level amounts to

$$p_{i \rightarrow f} = \frac{2\pi}{\hbar} \left| \left\langle \Psi_i \middle| z - z_f \middle| \Psi_f \right\rangle \right|^2 \quad (13)$$

where Ψ_i is an excited state, Ψ_f is a ground state and the z -axis connects the spatial position of the centers involved on a distance l between each other. Let us assume the existence of two potential wells, one for the photoinduced electron and another for the hole. The zero-order approximations of these states are solutions of Eq. (3) with different a , E and $U(\mathbf{r})$. According to the perturbation approach, the first-order approximation of states can be determined via isolated state functions $\Psi_i^{(0)}$ (initial state) and $\Psi_f^{(0)}$ (final state). Thus prior to calculate the probability of transition $i \rightarrow f$ (Eq. (13)) we determine the functions $\Psi_{i,f}$ via the isolated states functions $\Psi_{i,f}^{(0)}$:

$$\Psi_i = \Psi_i^{(0)} - \frac{1}{2} \left\langle \Psi_f^{(0)} \Psi_i^{(0)} \right\rangle \Psi_f^{(0)} \quad (14)$$

and

$$\Psi_f = \Psi_f^{(0)} - \frac{1}{2} \left\langle \Psi_i^{(0)} \Psi_f^{(0)} \right\rangle \Psi_i^{(0)} \quad (15)$$

We suppose that l is much larger than the sizes of the traps and the overlapping of initial and final states is very small. The seeking integral (13) can be taken with the considerations

$$\begin{aligned} \langle \Psi_j(r) | z | \Psi_f(r) \rangle &= \left\langle \Psi_j^{(0)}(r) | z | \Psi_f^{(0)}(r) \right\rangle - \frac{1}{2} \left\langle \Psi_j^{(0)}(r) \Psi_f^{(0)}(r) \right\rangle \\ &\quad \left(\left\langle \Psi_f^{(0)}(r) | z | \Psi_f^{(0)}(r) \right\rangle + \left\langle \Psi_j^{(0)}(r) | z | \Psi_j^{(0)}(r) \right\rangle \right) \end{aligned} \quad (16)$$

The supposed symmetry of the states $\Psi_i^{(0)}$ and $\Psi_f^{(0)}$ leads to the result

$$\left\langle \Psi_s^{(0)}(r) | z | \Psi_i^{(0)}(r) \right\rangle = \frac{l}{2} \quad (17)$$

and

$$\left\langle \Psi_f^{(0)}(r) | z | \Psi_f^{(0)}(r) \right\rangle = -\frac{l}{2}. \quad (18)$$

Taking into account that $\Psi_i^{(0)}(r, a_i, U_i) \propto \frac{e^{-\kappa r}}{\kappa r} \Big|_{\kappa r \rightarrow \infty}$ and that the final state function asymptotically fades much faster we come to the result

$$\left\langle \Psi_j^{(0)}(r) | z | \Psi_f^{(0)}(r) \right\rangle \sim e^{-\kappa r}, \quad (19)$$

and the probability for an electron transition (Eq. (13)) therefore attains the form

$$p_{i \rightarrow f} = \beta l^2 \exp(-2\kappa l), \quad (20)$$

where β is a proportionality coefficient and l is the distance between the trapped electron and a hole. Then let us estimate the probability for an electron to recombine with the main part of the surrounding holes. We take L as an average distance between a localized photoinduced electron and a neighbour hole. The actual counterpart holes are thus located within a spherical layer of the radius L with the thickness $(2\kappa)^{-1}$ with the hole concentration n_h . The probability for an electron transition to these holes amounts to

$$P_{i \rightarrow f} = \beta L^2 n_h \exp(-2\kappa L) \quad (21)$$

With the account that $n_h L = \text{const}$, $L_e \sim n^{-1/3}$ and Eq. (20) is rewritten as

$$P_{i \rightarrow f} = \gamma n_h^{1/3} \exp(-2\kappa' n_h^{-1/3}) \quad (22)$$

γ is a constant coefficient. Then we can determine the function of the relaxation law for the photoinduced electrons as

$$\frac{dn_e}{dt} = -\gamma n_e P_{i \rightarrow f}. \quad (23)$$

Assuming the concentration of electrons and holes is the same $n_e = n_h = n$ we come to the differential equation

$$\frac{dn}{dt} = -\gamma n^{4/3} \exp(-2\kappa' n^{-1/3}) \quad (24)$$

The substitution $u = n^{-1/3}$ leads to the equation

$$\frac{du}{dt} = \frac{\gamma}{3} \exp(-2\kappa' u) \quad (25)$$

With the analytical solution

$$\frac{1}{2\kappa'} \exp(2\kappa' u) = \frac{\gamma}{3} t + C, \quad (26)$$

where C is a constant determined by the initial conditions, and consequently

$$u = \frac{1}{2\kappa'} \ln \left(\frac{2\kappa' \gamma}{3} t + C \right). \quad (27)$$

Finally the concentration of photoinduced electrons attains the form

$$n(t) = (2\kappa')^3 [\ln(\alpha t + C)]^3, \quad (28)$$

where κ' and α are material parameters. As seen from Eq. (28) the electron concentration tends to zero with the time tending to the infinity in a rather slow manner. The main result of the derivations is the seeking intensity function $I(t) - dn/dt$:

$$I(t) \propto [\ln(\alpha t + C)]^{-4} \frac{1}{\alpha t + C}. \quad (29)$$

The temporal dependence (29) obtained in this simple model gives a straightforward and transparent explanation of the relaxation process observing as hyperbolic-like luminescence decay function.

4 Conclusions

The problem of solid-state material luminescence has an old history and is studied in detail especially for crystalline inorganic media [12–16]. In organic materials, a variety of effects is associated additionally with specific molecular structure [1]. As concerned with polymers the phenomenon of delayed photoluminescence can originate in general either from triplet–triplet recombination or from recombination of electron–hole pairs [17, 18]. Actually, the time-delayed luminescence of polymers at low temperatures is usually observed in thermoluminescence measurements [19, 20].

The electron–hole recombination process is deeply studied in solids and the effect is accompanied with an energy release obeying well-established temporal dependences. Surprisingly the compressed-hyperbola law is not explained up to now. The solution probably can be found in the account of the quantum tunnelling process [21, 22] quite similar to use in our model.

In the presented report we combine detailed inspection of luminescence properties of a polymer Polyamide-6 existing in two crystalline forms and theoretical analysis of a model describing the time-delayed luminescence in the material. The main point of this study is the revealing of the temporal dependence of the afterglow effect and its theoretical analysis. The time-delayed luminescence function was found to reproduce well-known empirical Becquerel law (compressed hyperbola). We relate this result to the process of radiation release owing to the photoinduced charge recombination in the situation of negligible charge diffusion and random spatial distribution of the charges.

In the theoretical approach we succeeded to build a simple model for localized recombination centers. The advantage of the model is an analytical solution which describes the Becquerel law in a concise expression. The model proposed describes only single electron energy state and does

not include the temperature dependence yet. In general we can formulate only that the temperature influences on the time-delayed luminescence via depopulation of the traps and quenching the radiating transitions of the photoinduced electrons. The revealed difference between the treated α and γ forms of PA-6 appeared in the temperature influence on the observed afterglow. A possible explanation is the variation of the trapped charges energy levels, and this question requires further clarification.

We could also note the modified hyperbola (Becquerel law) function looks very common for a wide class of materials of a rather different origin e. g. studied recently afterglow effect in synthetic opal [23].

Acknowledgements The authors wish to thank Prof. G. I. Dovbeshko, Prof. A. K. Kadashchuk and Prof. N. I. Ostapenko for helpful considerations and Dr. L. N. Bugayova for the PA-6 samples supply. This study was performed within the project “Photophysics of the processes of optical radiation interaction with photorefractive, solid-state and bio-organic media” by National Academy of Sciences of Ukraine.

References

1. H. Pope, C.E. Swenberg, *Electronic Processes in Organic Crystals*, 2nd edn. (Oxford University Press, Oxford, 1999).
2. Yu.V. Romanovskii, A. Gerhard, B. Schweitzer, U. Scherf, R.I. Personov, H. Bässler, Phosphorescence of π -conjugated oligomers and polymers. *Phys. Rev. Lett.* **84**, 1027–1030 (2000)
3. J. Partee, E.L. Frankevich, B. Uhlhorn, J. Shinar, Y. Ding, T.J. Barton, Delayed fluorescence and triplet-triplet annihilation in π -conjugated polymers. *Phys. Rev. Lett.* **82**, 3673 (1999)
4. W. Klöpffer, Luminescence of poly(n-vinyl-carbazole) films at 77 K. II. Kinetic model of exciton trapping and annihilation. *Chem. Phys.* **57**, 75–87 (1981)
5. D.R. Holmes, C.W. Bunn, D.J. Smith, The crystal structure of polycapromide: nylon 6. *J. Polym. Sci.* **XVII**, 159–177 (1955)
6. H.M. Heuvel, R. Huisman, Effects of winding speed, drawing and heating on the crystalline structure of nylon 6 yarns. *J. Appl. Polym. Sci.* **26**, 713–732 (1981)
7. N. Vasanthan, D.R. Salem, FTIR spectroscopic characterization of structural changes in polyamide-6 fibers during annealing and drawing. *J. Polym. Sci. B* **39**, 536–547 (2001)
8. M.V. Vasnetsov, V.V. Ponevchinsky, A.A. Mitryaev, D.O. Plutenko, Observation of room-temperature afterglow in polyamide-6 under UV excitation. *SPQEO* **22**, 333–337 (2019)
9. S.M. Aharoni, *N-Nylons, Their Synthesis, Structure and Properties* (John Wiley & Sons, New York, 1997), pp. 316–317
10. N.S. Allen, M.J. Harrison, Analysis of the fluorescent and phosphorescent species in nylon-6,6 in relation to aldol condensation products of cyclopentanone. *Eur. Polym. J.* **21**, 517–526 (1985)
11. M.N. Berberan-Santos, E.N. Bodunov, B. Valeur, Mathematical functions for the analysis of luminescence decays with underlying distributions: 2. Becquerel (compressed hyperbola) and related decay functions. *Chem.* **317**, 57–62 (2005)
12. T. Matsuzawa, A new long phosphorescent phosphor with high brightness. *J. Electrochem. Soc.* **143**, 2670 (1996)
13. F. Clabau, X. Rocquefelte, S. Jobic, P. Deniard, Mechanism of phosphorescence appropriate for the long-lasting phosphors Eu^{2+} -doped SrAl_2O_4 with codopants Dy^{3+} and B^{3+} . *Chem. Mater.* **17**, 3904 (2005)

14. T. Aitasalo, J. Hölsä, H. Jungner, M. Lastusaari, Mechanisms of persistent luminescence in Eu^{2+} , RE^{3+} doped alkaline earth aluminates. *J. Lumin.* **94–95**, 59 (2001)
15. H.F. Brito, J. Hölsä, T. Laamanen, M. Lastusaari, M. Malkamäki, L.C.V. Rodrigues, Persistent luminescence mechanisms: human imagination at work. *Opt. Mater. Express* **2**, 371 (2012)
16. V. Vitola, D. Millers, I. Bite, K. Smits, A. Spustaka, Recent progress in understanding the persistent luminescence in SrAl_2O_4 :EuDy. *Mater. Sci. Technol.* **35**, 1661–1677 (2019). <https://doi.org/10.1080/02670836.2019.1649802>
17. M. Yokoyama, S. Shimokihara, A. Matsubara, H. Mikawa, Extrinsic carrier photogeneration in poly-N-vinylcarbazole. III. CT fluorescence quenching by an electric field. *J. Chem. Phys.* **76**, 724 (1982)
18. B. Schweitzer, V.I. Arkhipov, H. Bässler, Geminate pair recombination in a conjugated polymer. *Chem. Phys. Lett.* **304**, 365 (1999)
19. I. Glowacki, Z. Szamel, The nature of trapping sites and recombination centres in PVK and PVK–PBD electroluminescent matrices seen by spectrally resolved thermoluminescence. *J. Phys. D Appl. Phys.* **43**(29), 295101 (2010)
20. A. Kadashchuk, Yu. Skryshevskii, A. Vakhnin, N. Ostapenko, Thermally stimulated photoluminescence in disordered organic materials. *Phys. Rev. B* **63**, 115205 (2001)
21. V. Pagonis, C. Kulp, C.-G. Chaney, M. Tachiya, Quantum tunneling recombination in a system of randomly distributed trapped electrons and positive ions. *J. Phys. Condens. Matter* **29**, 365701 (2017)
22. D.J. Huntley, An explanation of the power-law decay of luminescence. *J. Phys. Condens. Matter* **18**, 1359 (2006)
23. M.V. Vasnetsov, VYu. Bazhenov, V.V. Ponevchinsky, A.A. Mityaev, A.D. Kudryavtseva, N.V. Tcherniega, Spectralswitching in a time-delayed emission from synthetic opal. *Int. J. Photon. Opt. Technol.* **3**, 22–24 (2017)

Publisher's Note Springer Nature remains neutral with regard to jurisdictional claims in published maps and institutional affiliations.